International Journal of Geo-Information

MDPI

Article

Analyzing the Contribution of Human Mobility to Changes in Air Pollutants: Insights from the COVID-19 Lockdown in Wuhan

Jiansheng Wu [1,2], Yun Qian [1], Yuan Wang [1] and Na Wang [1,2,*]

[1] Key Laboratory for Urban Habitat Environmental Science and Technology, School of Urban Planning and Design, Peking University, Shenzhen 518055, China; wujs@pkusz.edu.cn (J.W.); qianyun1010@whu.edu.cn (Y.Q.); yuan_wang@pku.edu.cn (Y.W.)

[2] Key Laboratory for Earth Surface Processes, Ministry of Education, College of Urban and Environmental Sciences, Peking University, Beijing 100871, China

* Correspondence: anna_wang@pku.edu.cn

Abstract: During the COVID-19 lockdown in Wuhan, transportation, industrial production and other human activities declined significantly, as did the NO_2 concentration. In order to assess the relative contributions of different factors to reductions in air pollutants, we implemented sensitivity experiments by Random Forest (RF) models, with the comparison of the contributions of meteorological conditions, human mobility, and emissions from industry and households between different periods. In addition, we conducted scenario analyses to suggest an appropriate limit for control of human mobility. Different mechanisms for air pollutants were shown in the pre-pandemic, pre-lockdown, lockdown, and post-pandemic periods. Wind speed and the Within-city Migration index, representing intra-city mobility intensity, were excluded from stepwise multiple linear models in the pre-lockdown and lockdown periods. The results of sensitivity experiments show that, in the COVID-19 lockdown period, 73.3% of the reduction can be attributed to decreased human mobility. In the post-pandemic period, meteorological conditions control about 42.2% of the decrease, and emissions from industry and households control 40.0%, while human mobility only contributes 17.8%. The results of the scenario analysis suggest that the priority of restriction should be given to human mobility within the city than other kinds of human mobility. The reduction in the NO_2 concentration tends to be smaller when human mobility within the city decreases by more than 70%. A limit of less than 40% on the control of the human mobility can achieve a better effect, especially in cities with severe traffic pollution.

Keywords: nitrogen dioxide (NO_2); random forest; human mobility; contribution rate; air pollution; COVID-19 lockdown

Citation: Wu, J.; Qian, Y.; Wang, Y.; Wang, N. Analyzing the Contribution of Human Mobility to Changes in Air Pollutants: Insights from the COVID-19 Lockdown in Wuhan. *ISPRS Int. J. Geo-Inf.* **2021**, *10*, 836. https://doi.org/10.3390/ijgi10120836

Academic Editor: Wolfgang Kainz

Received: 21 October 2021
Accepted: 10 December 2021
Published: 17 December 2021

1. Introduction

In recent years, severe air pollution has killed many people, which has aroused concern [1]. The air pollution is a comprehensive result of meteorological conditions and human activities. Road traffic is deemed as an important source of NO_2 and $PM_{2.5}$ [2–4], and it also has a significant impact on the concentration of O_3.

After the COVID-19 outbreak in Wuhan in December 2019 [5,6], China activated a first-level public health emergency response in Wuhan on 23 January 2020, taking measures such as cancelling mass gatherings, reducing the frequency of bus services in the city and halting long-distance buses [7]. Therefore, transportation, industrial production and other urban activities fell sharply [8,9]. Moreover, the improvement in air quality emerged, as was reported that tropospheric NO_2 vertical column densities reduced by 22–67% over East China in the 2020 lunar new year holiday season compared with those in 2019 [10]. Not only in China [11–13], similar situations also occurred in many other areas such as South Korea [14], Western Europe [15], and the USA [16]. Although secondary pollution

sometimes enhanced during the COVID-19 lockdown in China, emissions of primary pollutants undoubtedly reduced [17].

Considering the impact of meteorological conditions and human activities on the air quality, many models such as Random Forest, Difference-in-differences (DID) and the Non-Linear Autoregressive Distributed Lag (NARDL) model have been employed to explain the connection between the COVID-19 lockdown and the reduction in air pollution [18–21]. Random Forest (RF) is an ensemble learning method, which consists of several simple decision trees [22]. RF samples with replacement, and constructs several subsets and outputs predictions by aggregating and averaging the individual predictions of each weak tree on the subset [23]. Thanks to its out-of-bag estimation, the random forest algorithm has the advantages of good generalization and simplicity regarding the ingestion of heterogeneous data [24,25].

Road transport, industries, and thermal power plants may cause a large amount of NOx emissions [26]. Previous research mainly focuses on the changes in air pollutants and other relative factors during the lockdown period, while few of them study the contribution rate of different pollution sources [27]. Although some people have conducted quantitative analysis on the influence of transportation, they always emphasize the periods before and after the COVID-19 lockdown and seldom compare the conditions with the same period in 2021 [18,28], when the government implemented regular epidemic prevention and control measures. Moreover, there is no tradeoff analysis between the decrease in pollutant concentration and the decrease in human mobility intensity, which is insufficient to guide the actual road traffic control.

Taking these into consideration, three questions are put forward in this paper. First, compared with the same periods in 2019 and 2021, how did the COVID-19 lockdown affect air pollutants? Second, what respective roles did meteorological conditions, human mobility and emissions from industry and households play in the change in the NO_2 concentration during different periods? Third, what is the relationship between the decrease in air pollutants and the reduction in human mobility? Is there a priority aspect with respect to human mobility control within the city, into of the city, and out of the city? What is the optimal extent for road traffic control? To answer these questions, we calculate the variation in air pollutants and related variables in Wuhan and employ stepwise regression models to detect the meaningful variables from 1 January to 16 March in 2020 and in the same period of the lunar calendar in 2019 and 2021. In addition, we operate nine sensitivity experiments to evaluate the contribution of meteorological conditions, human mobility and emissions from industry and households to the change in NO_2 concentrations. Finally, an emulator of change in human mobility as well as that in NO_2 concentration helps to identify the relationship between them and thus to find an effective way and a threshold level to reduce air pollution.

2. Materials and Methods

2.1. Research Area

Wuhan is an important industrial city in central China, with a population of 11 million. With the development of the economy, many large-scale air pollution events occur in Wuhan, which pose a significant threat to air quality [29]. Compared to other cities, it has relatively severe NO_2 pollution and stricter epidemic prevention and control.

Wuhan belongs to a typical subtropical monsoon climate with four clearly distinct seasons. The annual average temperature is 15.8–17.5 °C, and total annual precipitation in the city is 1050–2000 mm [30]. During the lockdown period (24 January–5 April) from 2017 to 2020, the mean temperature, wind speed and relative humidity were 9.24–11.2 °C, 2.41–2.93 m/s, and 73.1–78.36%, respectively [31].

2.2. Data Collection

2.2.1. Ground-Level Monitoring Data

The dataset of hourly concentrations of air pollutants was downloaded from the website https://quotsoft.net/air/ (accessed on 27 June 2021), a third-party website publishing air quality data crawled from China National Environmental Monitoring Center (Beijing, China, http://www.cnemc.cn/, accessed on 27 June 2021). The data are collected from ten national control points in Wuhan (Donghu Liyuan, Hanyang Yuehu, Hankou Huaqiao, Wuchang Ziyang, Qingshan Ganghua, Zhuankou Xinqu, Hankou Jiangtan, Wujiashan and 182 Minzu Avenue, with Chenhu Qihao as the reference site), the spatial distribution of which are depicted in Figure 1. The missing hourly value is replaced by the average value of other hours, and then the daily concentrations from ten sites are calculated and averaged into daily means of Wuhan.

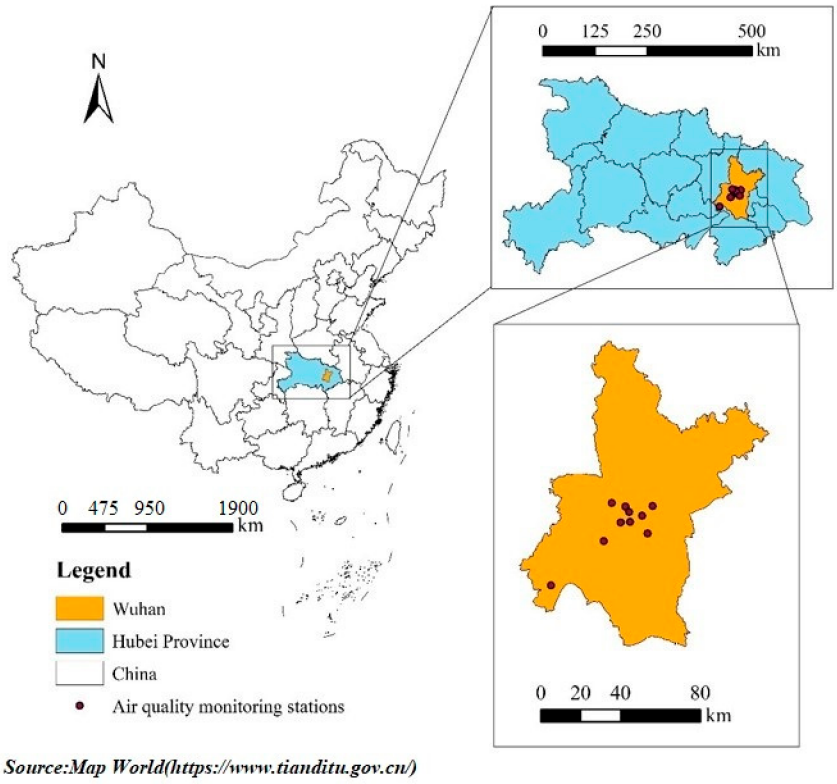

Figure 1. Locations of monitoring stations.

2.2.2. Human Activities

Compared with other air pollutants, the NO_2 concentration is more directly connected to anthropogenic factors, among which the road transport emissions are important contributors [32,33]. The daily migration dataset was obtained from Baidu Migration Platform to show the real-time information about human mobility [34]. The daily In-Migration Index (IMI) and Out-Migration Index (OMI) were chosen to represent the inflow and the outflow traffic volume of Wuhan, and the daily Within-City Migration Index (WMI) to represent human traffic mobility in Wuhan [20]. The IMI and OMI are the indexed results of the ratio of the number of people who have moved into and out of Wuhan to the total number of residents in Wuhan. The WMI represents the indexation result of the ratio of the number of people traveling in Wuhan to the total resident population in Wuhan [27].

The concentration ratio of NO_2 and SO_2 is commonly used to represent the change in contribution rate of mobile emission source and fixed emission source of air pollutants [35]. As a reflection of the characteristics of the energy structure, regions which emit mainly SO_2 have developed industries [36]. According to the Bulletin of the second national survey of

pollution sources in Wuhan, nitrogen oxide mainly comes from industrial, households and mobile sources while SO_2 mainly comes from industry and households (Table 1). Therefore, we employ SO_2 as a proxy of the level of emissions from industrial and households.

Table 1. The proportions of air pollutants from different sources in Wuhan.

Different Sources	Sulfur Dioxide (SO_2)	Nitrogen Oxides (NO_x)	Particulate Matter
Industrial sources	38.36%	37.96%	56.16%
Household sources	61.37%	4.66%	41.42%
Mobile sources	0.00%	57.19%	2.28%
Others	0.27%	0.19%	0.14%

2.2.3. Meteorological Data

The daily surface climate dataset of Wuhan was downloaded from the China meteorological science data sharing service network (http://data.cma.cn, accessed on 1 July 2021). Six meteorological variables are considered in our models, including precipitation (prep), air pressure (pressure), temperature (temp), relative humidity (RH), maximum wind speed (ws) and maximum wind direction (wd), which have been verified to be closely linked with the NO_2 concentration [37].

2.3. Methods

First, to identify the pollution mechanisms during four periods, including the pre-pandemic period (12 January to 28 March 2019), pre-lockdown period (1 January to 22 January 2020), lockdown period (24 January to 16 March 2020), and post-pandemic period (19 January to 4 April 2021), we fitted the NO_2 concentration in each period with stepwise regression models and identified meaningful variables. Second, we fitted the NO_2 concentration during the pre-pandemic period with Random Forest models and computed the relative contributions of meteorological conditions, human mobility, emissions from industry and households to the changes of NO_2 concentration through three groups of nine sensitivity experiments. Third, we employed Random Forest models to simulate the changes of pollutant concentrations with the decrease in human mobility in different scenarios for road traffic control. The flowchart of methodology is illustrated in Figure 2.

2.3.1. Random Forest Models

We employ Random Forest models to conduct regression analysis to fit NO_2 concentrations in the pre-pandemic period. Two important parameters should be considered carefully in the random forest algorithm [38]. The parameter mtry determines the variable sampling value of each iteration and the number of variables sampled to grow each leaf within a tree. The parameter ntree specifies the number of decision trees contained in the Random Forest, which is 500 by default. Ten-fold validation is operated in the model and the most appropriate value of mtry and ntree is chosen by grid search to pursue the minimum R-squared of the model. The Random Forest model is operated by package "Caret" in R version 3.6.1.

Apart from the variables about meteorological conditions, human mobility and emission sectors, time variables are also included in the model. The variable week means the day of the week, ranging from 1 to 7 and the variable Julian means the day of a year. Since the Spring Festival effect is an important issue in the study of air pollution, the variable lunar, which means the number of days after the first day of the Lunar New Year holiday is used to reflect changes in air pollutants before and after the Spring Festival holiday [18,39]. For example, the Spring Festival in 2019 is on 5 February, so the value the variable lunar is -1, 0 and 1 for 3, 4, and 5 February, respectively. The variable lunar is 0 on 25 January 2020 and on 12 February 2021, the days when the Spring Festival holiday begins in 2020 and 2021.

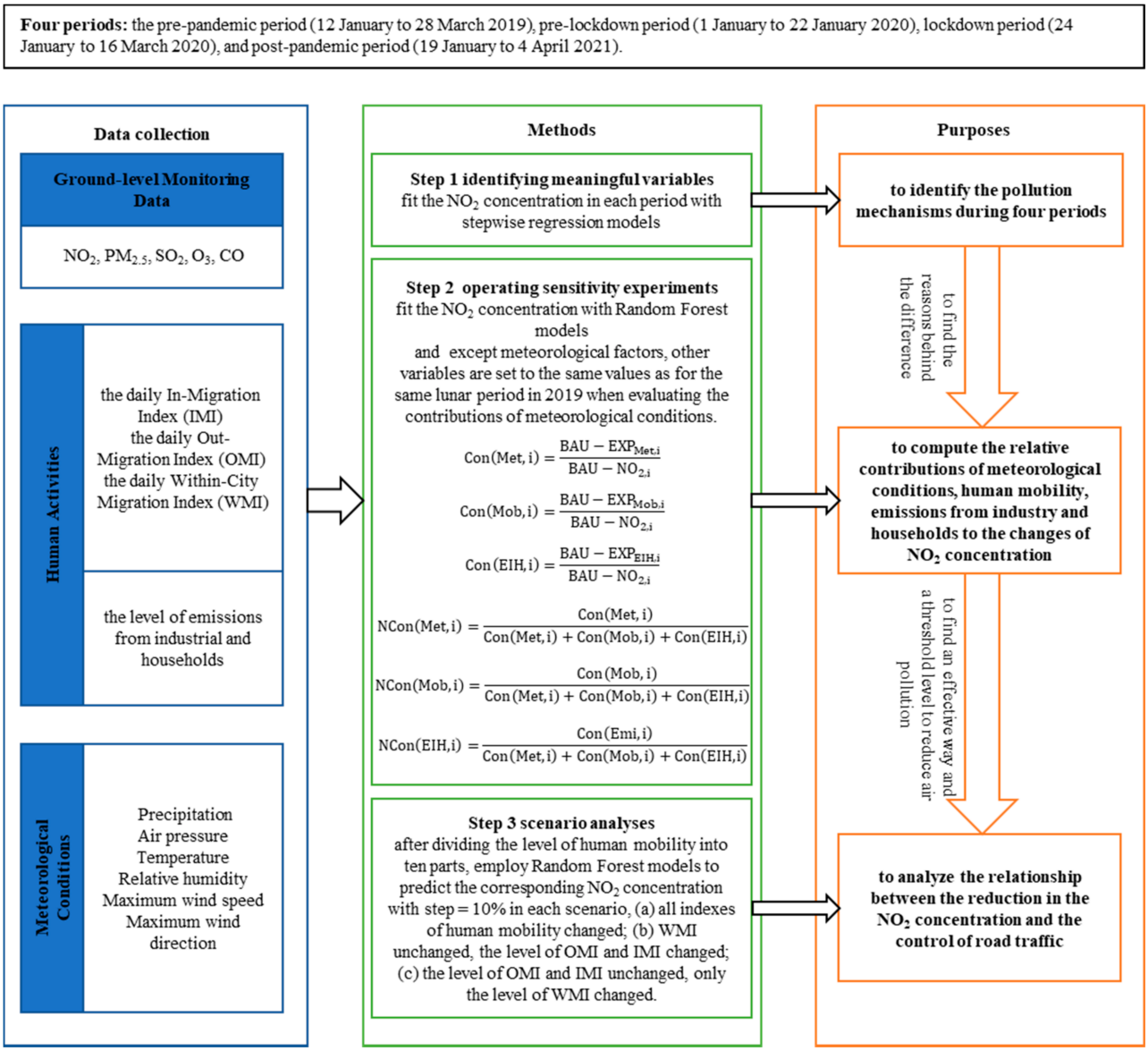

Figure 2. The flowchart of methodology.

2.3.2. Sensitivity Experiments

We performed nine experiments to quantify the contributions of meteorological conditions ($EXP_{Met,i}$), human mobility ($EXP_{Mob,i}$) and emission from industry and households ($EXP_{EIH,i}$) to the changes of NO_2 during the pre-lockdown, lockdown and post-pandemic period, respectively [40] (see Table 2). For example, under the assumption that the level of the NO_2 concentrations without the change of the specific variables will be similar to that in 2019, except meteorological factors, other variables are set to the same values as for the same lunar period in 2019 when evaluating the contributions of meteorological conditions. The NO_2 concentration during the pre-pandemic period in 2019 is recorded as business as usual (BAU), and the NO_2 concentrations in other three periods are recorded as $NO_{2,i}$, in which $i = 1$ means the pre-lockdown period, $i = 2$ means the lockdown period and $i = 3$ means the post-pandemic period. The contributions of factors and the normalization process are calculated as follows,

$$Con(Met, i) = \frac{BAU - EXP_{Met,i}}{BAU - NO_{2,\,i}}, \quad (1)$$

$$Con(Mob,i) = \frac{BAU - EXP_{Mob,i}}{BAU - NO_{2,i}}, \quad (2)$$

$$Con(EIH,i) = \frac{BAU - EXP_{EIH,i}}{BAU - NO_{2,i}}, \quad (3)$$

$$NCon(Met,i) = \frac{Con(Met,i)}{Con(Met,i) + Con(Mob,i) + Con(EIH,i)}, \quad (4)$$

$$NCon(Mob,i) = \frac{Con(Mob,i)}{Con(Met,i) + Con(Mob,i) + Con(EIH,i)}, \quad (5)$$

$$NCon(EIH,i) = \frac{Con(Emi,i)}{Con(Met,i) + Con(Mob,i) + Con(EIH,i)}, \quad (6)$$

$Con(Met,i)$, $Con(Mob,i)$ and $Con(EIH,i)$ modeled the contributions of meteorological conditions, human mobility and emissions from industry and households, with the normalized contributions represented by $NCon(Met,i)$, $NCon(Mob,i)$ and $NCon(EIH,i)$.

Table 2. Design of the sensitivity experiments.

Experiment	Description
$EXP_{Met,i}$	The simulated NO_2 concentrations in RF model run with meteorological variables in i [1] period and other variables in 2019.
$EXP_{Mob,i}$	The simulated NO_2 concentrations in RF model run with variables about road traffic in i [1] period and other variables in 2019.
$EXP_{EIH,i}$	The simulated NO_2 concentrations in RF model run with variables about emissions of industry and households in i [1] period and other variables in 2019.

[1] i = 1 means the pre-lockdown period, i = 2 means the lockdown period and i = 3 means the post-pandemic period.

2.3.3. Scenario Analysis

We operated an emulator to analyze the relationship between the reduction in the NO_2 concentration and the control of road traffic [28]. The level of road traffic in 2019 is deemed as the pre-pandemic level and three series of scenarios are set, (a) all indexes of human mobility changed; (b) Within-City Migration Index unchanged, the level of Out-Migration and In-Migration changed; (c) the level of Out-Migration and In-Migration unchanged, only the level of Within-City Migration Index changed.

First, after dividing the level of human mobility into ten parts, we employed Random Forest models to predict the corresponding NO_2 concentration with step = 10% in each scenario. Second, we further calculated the change rate of the NO_2 concentrations for each ten percent of the level of human mobility index. Third, we compared the change rate and the decline rate to see whether the control of specific human mobility index was inhibitory to the NO_2 concentrations. Finally, when the change rate of the NO_2 concentrations was mostly equal to 0 (above 50% probability), we considered that the current effect of human mobility control reached a threshold level.

3. Results

3.1. Different Mechanisms in Different Periods

The change in NO_2 concentration was the most prominent. The average NO_2 concentrations for the pre-lockdown and lockdown periods in 2020 were 42.04 and 19.75 $\mu g/m^3$, compared with 55.99 and 42.84 $\mu g/m^3$ for the same lunar calendar periods in 2019 and 48.87 and 35.22 $\mu g/m^3$ in 2021, showing that the air pollution significantly decreased in 2020 and rebounded slightly in 2021. Similar to the abovementioned trend, for the pre-lockdown period, average $PM_{2.5}$ concentrations were 96.68, 60.60, 65.98 $\mu g/m^3$ and average SO_2 concentrations were 9.92, 6.83, 8.29 $\mu g/m^3$ in 2019, 2020 and 2021. For the lockdown period, average $PM_{2.5}$ concentrations were 55.70, 38.61, 39.06 $\mu g/m^3$ and average SO_2 concentrations were 8.31, 7.57, 7.75 $\mu g/m^3$ in 2019, 2020 and 2021. In contrast with the NO_2 concentrations, the average O_3 concentrations increased in 2020 and then

dropped in 2021, with 41.26, 59.67, 48.28 $\mu g/m^3$ for the lockdown period in each year. The average CO concentrations showed a slight decreasing trend over three years, with 0.95, 0.91, 0.78 mg/m^3 for the lockdown period in each year.

As is shown in Figure 3, it is obvious that the NO_2 and $PM_{2.5}$ concentration dropped sharply after the lockdown began in Wuhan (23 January 2020), while the O_3 concentration obviously increased. There was an inverse relationship between the amount of NO_2 and ozone [41]. During the first week after the Spring Festival, the CO, NO_2, $PM_{2.5}$, and SO_2 concentrations significantly decreased. The difference between the NO_2 concentration in 2020 and in 2019 during the week after 30 January reached a relatively small value as the enterprises offering protective products and emergency supplies resumed work and production. In the pre-pandemic period in 2019, the NO_2 concentration rebounded slowly after the Spring Festival. However, in 2020, it kept a low level even after the Spring Festival, showing a close correspondence with the COVID-19 lockdown. Meanwhile, the concentrations of the two pollutants in 2021(the post-pandemic period) were still lower than that in 2019. The change in NO_2 concentration was most prominent, dropping by 24.9% in the pre-lockdown period, 53.9% in the lockdown period and 15.4% in the post-pandemic period in 2021, compared to the pre-pandemic period.

The meteorological conditions for different periods over the three years are listed in Table 3, and the changes in human mobility over the same periods are illustrated in Figure 4. The meteorological conditions changed a little. During the lockdown period, the average pressure (pressure) and wind direction (wd) in 2020 were higher than those in 2019 and 2021 while the average wind speed (ws) was lower than those in 2019 and 2021.

Table 3. Descriptive statistics of meteorological conditions over three years. (prep, pressure, temp, RH, ws, and wd represent precipitation, air pressure, temperature, relative humidity, maximum wind speed and maximum wind direction, respectively.).

Property		The Pre-Lockdown Period			The Lockdown Period		
		2019	2020	2021	2019	2020	2021
prep (mm)	Mean	1.4	4.5	1.68	2.25	2.61	3.93
	Median	0	0.2	0.85	0	0	0
	Std.	3.72	9.18	2.35	3.85	7.81	7.83
pressure (hPa)	Mean	1020.44	1022.84	1020.6	1018.98	1020.76	1015.85
	Median	1023.9	1022.65	1020.45	1019.1	1021.8	1016.7
	Std.	4.2	2.77	2.81	5.96	5.64	6.16
temp (°C)	Mean	4.46	4.03	7.27	8.25	8.79	12.22
	Median	4.95	4.15	7.7	8.5	8.9	11.8
	Std.	2.3	2.03	1.54	5.06	4.04	3.39
RH (%)	Mean	79.53	86.51	86.24	82.09	80.58	79.86
	Median	83.65	87.65	88.75	84.5	81.5	83.5
	Std.	12.06	8.07	7.4	10.35	7.9	11.65
ws (m/s)	Mean	3.92	3.45	3	4.02	3.89	4.23
	Median	3.2	3.4	2.65	3.9	3.5	4.1
	Std.	1.62	1.07	1	1.56	1.37	1.27
wd (°)	Mean	128.27	155.64	136.95	145.21	154.42	131.7
	Median	106	78.5	121.5	107	125	102
	Std.	119.62	143.3	112.83	128.55	119	116.63

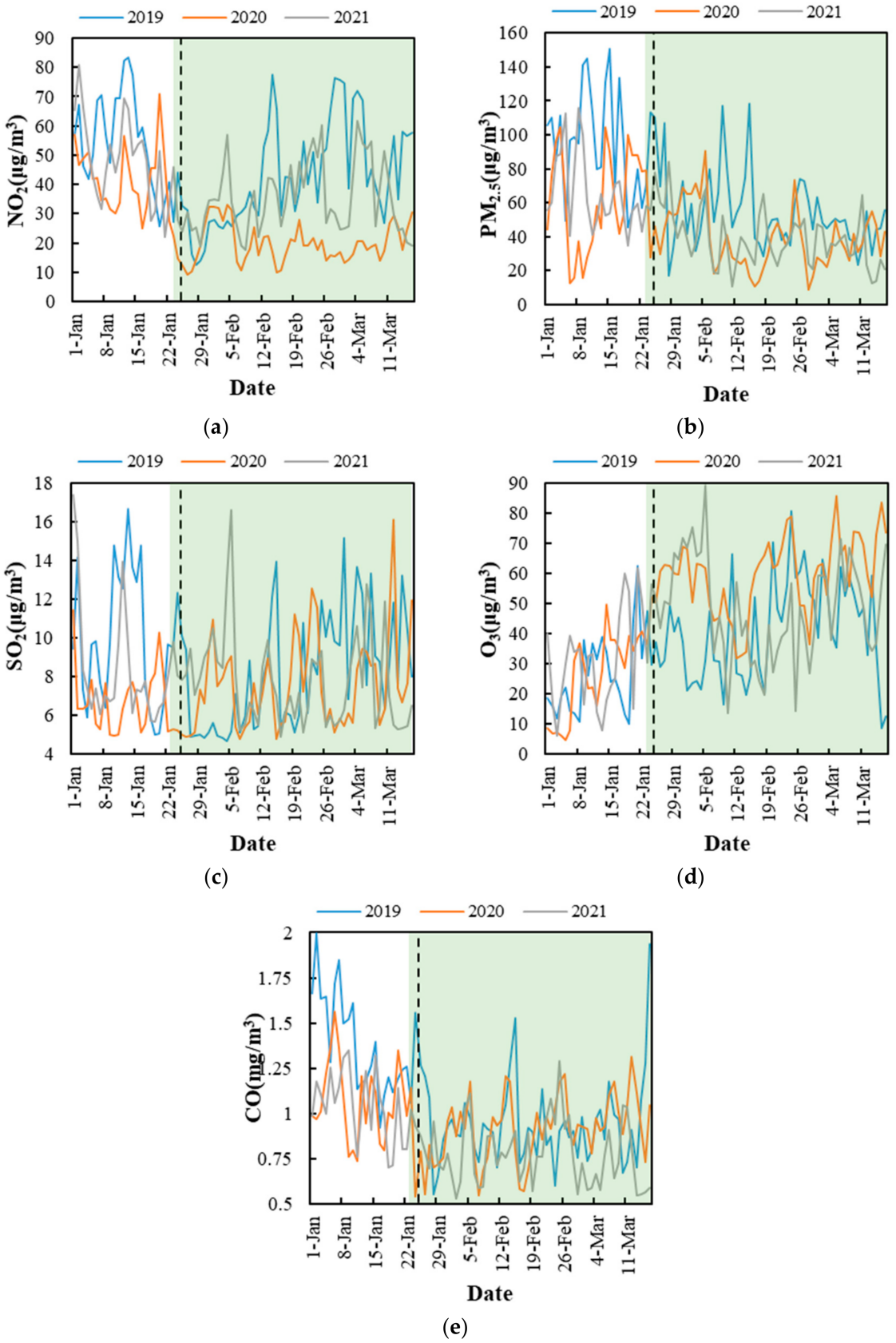

Figure 3. Observed changes in air pollutants over three years: (**a**) NO_2; (**b**) $PM_{2.5}$; (**c**) SO_2; (**d**) O_3; (**e**) CO (The black dashed vertical line means the date of the Spring Festival and the green area means the lockdown period in our study.).

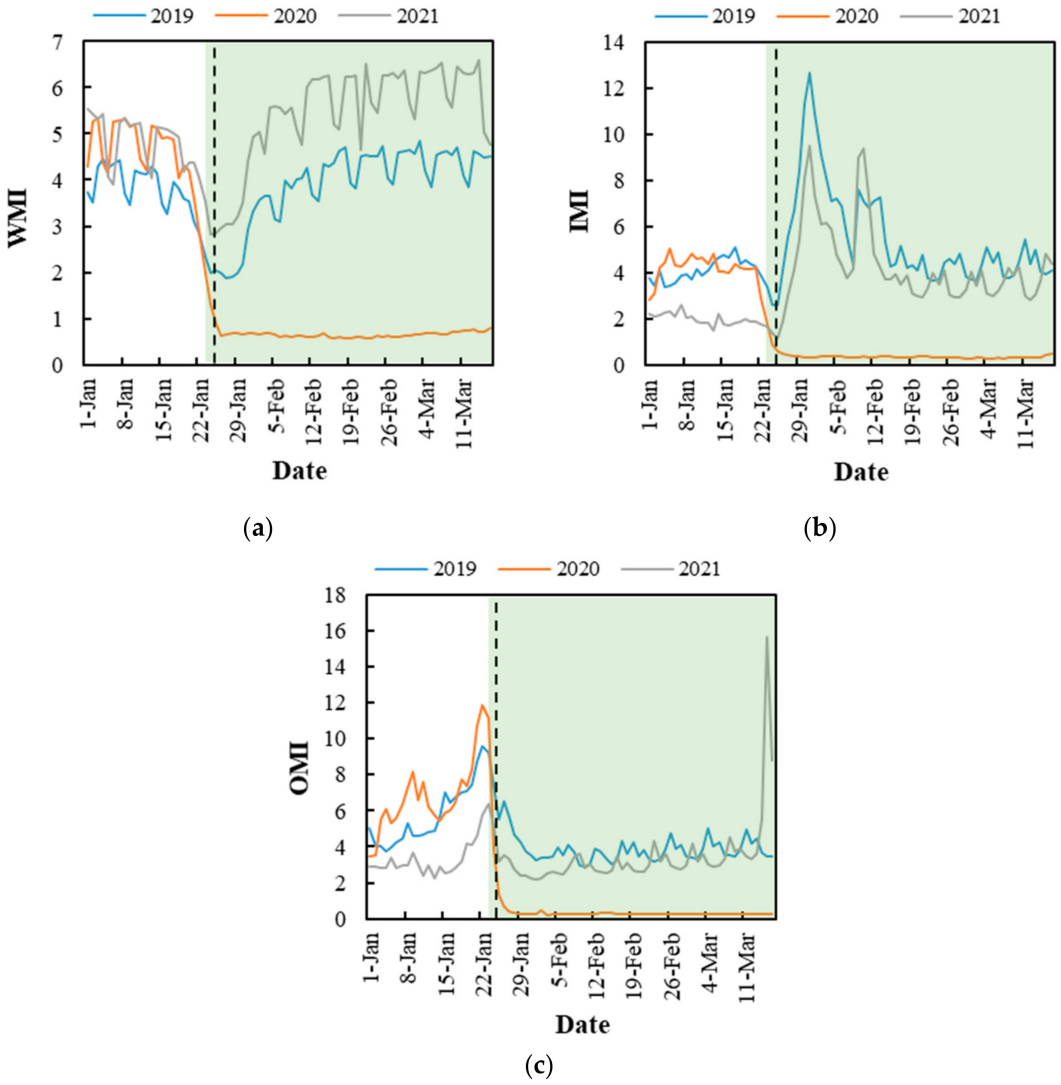

Figure 4. Changes in human mobility over three years: (**a**) WMI; (**b**) IMI; (**c**) OMI (The black dashed vertical line means the date of the Spring Festival and the green area means the lockdown period in our study. The daily In-Migration Index (IMI) and Out-Migration Index (OMI) represent the inflow and the outflow traffic volume, and the daily Within-City Migration Index (WMI) represents human traffic mobility within the city).

There are obvious trends in the variables about human mobility. The average WMI, IMI, OMI during the lockdown period in 2020 were 0.66, 0.37, and 0.37, respectively, much lower than those in 2019 (3.89, 5.43, and 3.93) and in 2021 (5.43, 4.26, and 3.48). The Spring Festival holiday usually results in the decrease in $PM_{2.5}$ and NO_2 and an increase in ozone in big megacities [42] because many people return to their hometowns [43,44]. The changes in air pollutants are the comprehensive results of the holiday effect and the pandemic control policies [45]. At the beginning of the Spring Festival migration in 2020 (10 January), the values of the WMI, IMI and OMI were higher than those in 2019. As can be seen from Figure 4c, a large number of people left Wuhan a few days before the lockdown, which was more than the number in 2019. Even on 23 January 2020 (on which day 10:00 a.m. was Wuhan's lockdown time), the number of people leaving Wuhan on that day was higher than that on the same day of the lunar calendar in 2019. When Wuhan undertook the COVID-19 lockdown policy, the flow of persons was reduced to zero and the IMI decreased. Different from that, indexes rebounded after the first week of the holiday of the Spring Festival in 2019 and 2021, the levels of human mobility in 2020 remained at a low level because of the COVID-19 lockdown.

In addition, the average WMI during the post-pandemic period in 2021 was 5.23, higher than 3.85 during the pre-pandemic period in 2019, while the average IMI and OMI were 3.57 and 3.44, both less than 5.03 and 4.50 in 2019. We can notice that in 2021, when the epidemic prevention and control was regular, the travel intensity of residents in the city increased, while the activities of moving into the city and moving out of the city decreased compared with pre-pandemic conditions, with most of residents traveling in the city. Notably, there was a high value of WMI on 3 April 2021, corresponding to the first day of the Tomb Sweeping Day holiday.

Different mechanisms are illustrated over four periods. The stepwise regression model of the pre-pandemic period included four explanatory variables, which explained 82.8% of the variance of the NO_2 concentration. The stepwise regression model of the pre-lockdown, the lockdown and the post-pandemic period included one, one, and four explanatory variables, respectively, and each explained 54.0%, 47.6% and 63.9% of the variance of the NO_2 concentrations.

The regression coefficients of the models are shown in Table 4. The explanatory variables significantly affect the NO_2 concentrations ($p < 0.01$). It is obvious that emissions from industry and households (represented by SO_2) are closely connected with the NO_2 concentration and have a positive impact on it whichever period. The wind speed (ws) had a lowering effect on the NO_2 concentration in the pre-pandemic and post-pandemic period, showing the impact of meteorological elements. The models in the pre-pandemic and post-pandemic period were more similar, while the Within-City Migration Index played a more important role in the post-pandemic period. The NO_2 concentrations in the pre-lockdown and lockdown period fluctuated largely and the Within-City Migration Index and wind speed were meaningless in the two periods.

Table 4. Regression coefficients of stepwise multiple linear models over four periods.

Periods	Property	Unstandardized Coefficients		Standardized Coefficients
		B	Std. Error	
The pre-pandemic period	(Constant)	−7.188	5.221	
	SO_2	3.910	0.286	0.694
	WMI	9.902	1.288	0.432
	ws	−2.708	0.568	−0.236
	julian	−0.163	0.045	−0.200
The pre-lockdown period	(Constant)	9.938	6.827	
	SO_2	4.700	0.971	0.735
The lockdown period	(Constant)	5.632	2.173	
	SO_2	1.866	0.274	0.690
The post-pandemic period	(Constant)	15.278	6.787	
	SO_2	2.341	0.405	0.431
	ws	−4.097	0.830	−0.380
	WMI	6.448	1.218	0.462
	julian	−0.221	0.060	−0.344

3.2. Relative Contributions of Meteorological Conditions and Human Activities

We used a Random Forest model to fit the NO_2 concentrations during the pre-pandemic period, along with a Support Vector Machine model, a Linear model and a Stepwise Multiple Linear model to evaluate the performance. The four models all had high accuracy, the smallest cross-validation R-squared (CV-R^2) of which was 0.771. Other goodness indicators are shown in Table 5. Overall, all the simulation results were acceptable, and the simulated concentrations agreed well with the observed data, with the correlation coefficient (COR) above 0.9 for each model.

Table 5. Models and performance evaluation. (CV-R^2, COR, R^2, RMSE, MAE, NMB and NME mean the cross-validation R-squared, the correlation coefficient, R-squared, the root mean square error, the mean absolute error, the normalized mean bias, and the normalized mean error, respectively).

Model	CV-R^2	COR	R^2	RMSE	MAE	NMB	NME
Random Forest	0.771	0.984	0.968	4.493	3.632	0.039	7.821
Support Vector Machine	0.826	0.967	0.934	0.934	3.109	−1.307	6.695
Linear	0.798	0.917	0.841	7.146	5.276	0.000	11.361
Stepwise Multiple Linear Model	0.844	0.910	0.828	7.441	5.628	0.000	12.120

We employed Random Forest models to operate sensitivity experiments and then calculated the relative contributions of meteorological conditions and human activities for different periods. The results are shown in Table 6 and Figure 5. The contributions of meteorological conditions and human activities varied from day to day, and we calculated the average NO_2 concentration and the average contributions during the whole period. In the pre-lockdown period, the NO_2 concentration simulated with human mobility in 2020 was more similar to the NO_2 concentration in the pre-pandemic period than that simulated with meteorological conditions and emissions from industry and households in 2020, which means that road traffic led to the least contribution to the change of air pollutants and the changed emissions from industry and households contributed the most. The mean values of the daily normalized contribution were 35.2%, 13.8% and 51.0% for $NCon(Met)$, $NCon(Mob)$ and $NCon(EIH)$. During the first week of the pre-lockdown period, changes in meteorological conditions made the greatest contributions to the daily reductions in the concentrations. During the last two weeks of this period, the reduction in emissions from industry and households played the most important role in the reduction in the concentrations.

Table 6. The observed concentrations and the simulated results of sensitivity experiments (unit: $\mu g/m^3$).

Periods	Average Observed NO_2	Average Observed NO_2 during the Pre-Pandemic Period in 2019	Average $EXP_{Met,i}$	Average $EXP_{Mob,i}$	Average $EXP_{EIH,i}$
The pre-lockdown period	42.04	55.99	52.19	54.73	50.02
The lockdown period	19.75	42.84	45.34	40.14	41.74
The post-pandemic period	39.31	46.44	47.34	46.79	44.70

During the lockdown period, the observed NO_2 concentrations were lower than those in the pre-pandemic period in 2019 except for the days between 28 January and 5 February (when the variable lunar is between 4 and 12). The average NO_2 concentration simulated with meteorological conditions in 2020 was higher than the observed NO_2 concentrations in the same period in 2019, indicating that the meteorological conditions during the lockdown period essentially were unfavorable to the reduction in the air pollutants. The average NO_2 concentration simulated with human mobility in 2020 was the lowest, which means that road traffic dominated the reduction in the NO_2 concentration during the lockdown period. In addition, the average normalized contributions of $NCon(Met)$, $NCon(Mob)$ and $NCon(EIH)$ were, respectively, 10.0%, 73.3% and 16.7%, which emphasized the role of human mobility again. The changes in road traffic dominated changes of the concentration during the third, fourth, and last week of the lockdown period.

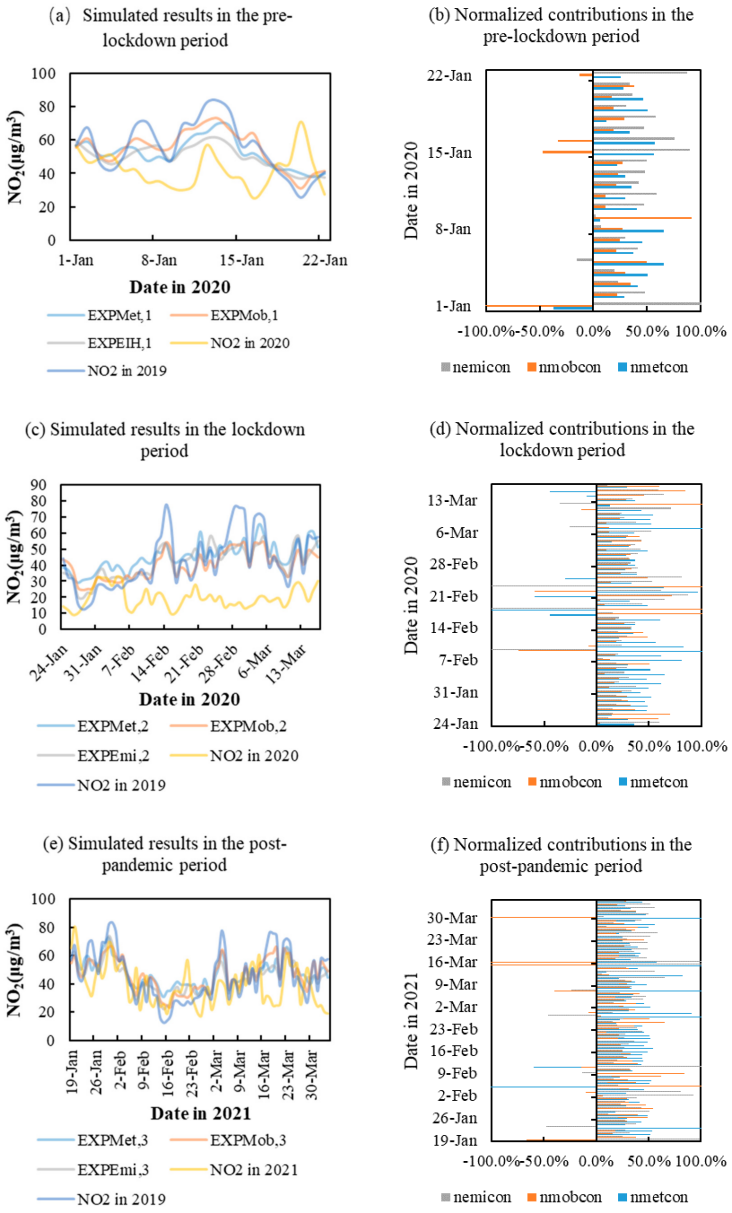

Figure 5. The simulated NO_2 concentrations and the normalized contributions in three periods: (**a**) Simulated results in the pre-lockdown period; (**b**) Normalized contributions in the pre-lockdown period; (**c**) Simulated results in the lockdown period; (**d**) Normalized contributions in the lockdown period; (**e**) Simulated results in the post-pandemic period; (**f**) Normalized contributions in the post-pandemic period. $(NCon(Met,i)$, $NCon(Mob,i)$ and $NCon(EIH,i)$ mean the normalized contributions of meteorological conditions, human mobility and emissions from industry and households. $EXP_{Met,i}$ means the simulated NO_2 concentrations in RF model run with meteorological variables in i period and other variables in 2019; $EXP_{Mob,i}$ means the simulated NO_2 concentrations in RF model run with variables about road traffic in i period and other variables in 2019; $EXP_{EIH,i}$ means the simulated NO_2 concentrations in RF model run with variables about emissions of industry and households in i period and other variables in 2019, where i = 1 means the pre-lockdown period, i = 2 means the lockdown period and i = 3 means the post-pandemic period).

During the post-pandemic period, the average observed NO_2 concentration was still less than that during the same period in 2019, mostly due to emissions from industry and households. The NO_2 concentration simulated with meteorological conditions in 2021 was higher than that in 2019, which shows that the general meteorological elements in the post-

pandemic period in 2021 are favorable to the increase in the NO_2 concentration. Moreover, the level of road traffic recovered to the pre-pandemic level, with the NO_2 concentration simulated with human mobility in 2021 being similar to that in 2019. According to the normalization process, the meteorological conditions controlled about 42.2% of the decrease, and the reduced emissions from industry and households controlled 40.0% of the decrease, while the level of human mobility only contributes to 17.8% of the decrease. As was shown in Figure 5f, in the post-pandemic period, the NO_2 concentrations do not completely show a downward trend compared with the same period in 2019, and the contribution rate of variables varies greatly from day to day. When the variable lunar was −6 (5 February 2021), meteorological conditions led to an increase of 490.4% of pollutants, while human mobility led to a decrease of 569.4% of concentration. When the variable lunar was 32, 33 and 47 (15, 16, and 30 March 2021), human mobility led to an increase of 799.5%, 117.2% and 126.0% of concentration, while meteorological conditions were conducive to the reduction in pollutants.

3.3. Simulations of Different Scenarios for Road Traffic Control

The emulator demonstrates the link between NO_2 concentrations and road traffic by predicting the concentrations with different reductions in human mobility compared to the level in 2019 in three scenarios. As shown in Figure 6, all the changes tend to approach a stable level when the reduction in human mobility continues. According to the variation rate of the NO_2 concentrations, for the three scenarios, all the change rates are very large at the beginning, but with the reduction in human mobility, the variation rate becomes gradually flat. This means the control of human mobility has a stronger effect at the beginning, with a gentler change trend later. Generally, in Figure 6c, when human mobility within the city is controlled, the decreasing trend is almost constant whatever the basic NO_2 concentration. In Figure 6a, bscenario (a) and (b), only when the initial basic NO_2 concentration is relatively high, the NO_2 concentration will remain decreased with the level of human mobility within the city reduced.

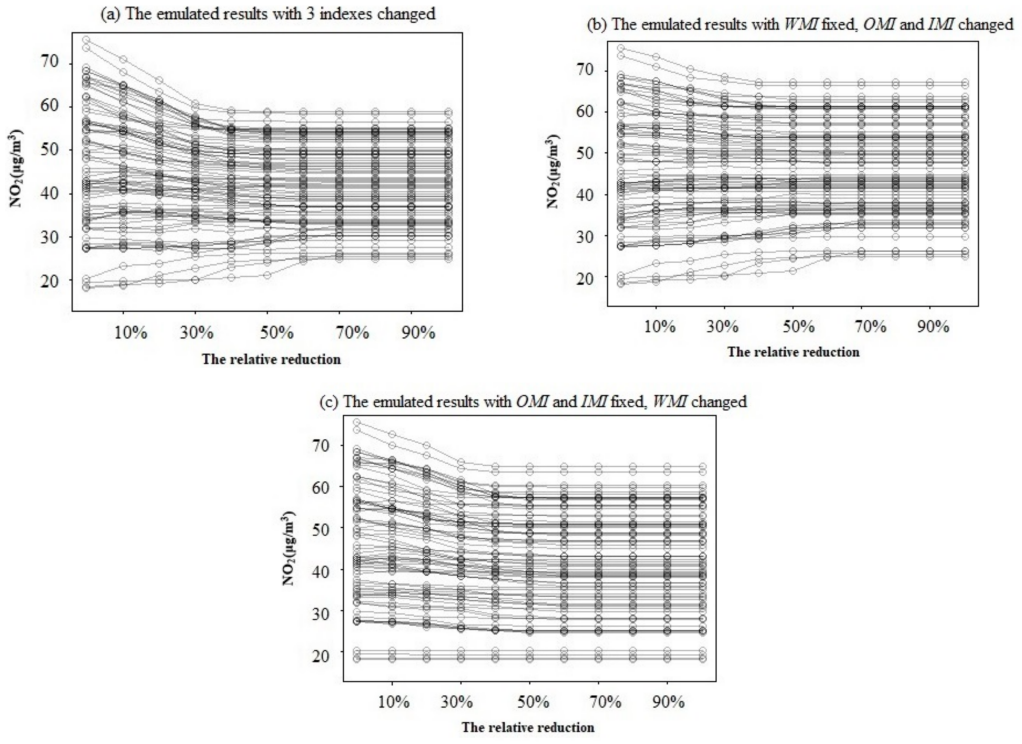

Figure 6. The simulated results of the decreased road traffic and the NO_2 concentration: (**a**) 3 indexes changed; (**b**) WMI fixed, OMI and IMI changed; (**c**) OMI and IMI fixed, WMI changed).

When the reduction in all kinds of human mobility is beyond 70%, the effect of the control policy reaches a threshold level. This means that when the proportion of the overall human mobility is less than 30% of the pre-pandemic level, the pollutant concentration will remain stable. When we control the human mobility out of and into the city and leave the mobility within the city unchanged, the threshold level is 60%, and when we only control the mobility within the city, the threshold level is 70%, which indicates that the control policy in Figure 6b is less sustainable. Moreover, the variation rate is less than 10 when the reduction in human mobility is more than 40% both in Figure 6a,c, while the variation rate in Figure 6b is less than 10 when the reduction in human mobility is more than 20%. We can conclude that controlling the human mobility within the city is more effective than controlling the mobility out of and into the city, and the effect of the former policy almost equals that of taking an overall control of all kinds of human mobility.

4. Discussion

4.1. Contributions of Meteorological Conditions and Emissions during Different Periods

The RF models have good accuracy as an atmospheric physical transport model, compared with the validation parameters in other studies [40]. Assessing meteorological differences is important because similar meteorological conditions usually accompany similar NO_2 levels [46]. As for meteorological conditions, the importance of wind speed is emphasized in Table 4. Wind speed affects the horizontal diffusion of pollutants [47]. The average wind speed in 2020 was lower than that of the pre-pandemic period, which would have increased the NO_2 concentration. Previous studies find that pressure, relative humidity and temperature play an important role in pollutant concentrations. High pressure may decelerate the diffusion of pollutants while high relative humidity is also helpful to eliminate NO_2 [48,49]. During the lockdown period in 2020 (Table 3), the average pressure was the highest, and the average relative humidity was relatively low, which was unfavorable to the reduction in the NO_2 concentration. In addition, the NO_2 concentrations are much higher in the cool season [50]. During the pre-lockdown period, the temperature was relatively low, while during the lockdown period, the temperature was higher than that in the pre-pandemic period. Despite all those negative effects on reduction, the NO_2 concentrations 2020 were lower than that in the pre-pandemic period, which reflected that road traffic dominated the reduction in the NO_2 concentration during the lockdown period (contributing 73.3% to the reduction), while the meteorological conditions contributed the least (only 10.0%).

The NO_2 concentration is closely tied to the volume of traffic, fossil fuel use and emission by industrial activities. During the pre-lockdown period, the normalized contribution of human mobility and emissions from industry and households to the reduction was 13.8% and 51.0%. However, during the lockdown period, human mobility contributed 73.3% to the reduction, which emphasizes the role of traffic control measures. During the post-pandemic period, human mobility only contributed to a 17.8% decrease. On one hand, compared to the lockdown period, the traffic control measures are weaker, and people can go outside within the city or travel between cities with their health passes. That is why human mobility contributes much less than during the lockdown period. On the other hand, when the government takes regular epidemic prevention and control measures in 2021, although the number of people moving out of and into the city became less, the number of people who moved within the city was larger than during the pre-pandemic period (Figure 4), which indicates the role of human mobility within the city in pollutants concentrations.

4.2. Insights for the Control of Human Mobility

Since traffic plays an important role in the NO_2 pollution, actions should be taken to set traffic restrictions to improve air quality. Many cities such as Amsterdam [51], Berlin [52] and Madrid [53] in Europe and Nanchang [54] in China have adopted policies of creating a low-emission zone (LEZ) area, with different levels of rules with regard to access to the

restricted area, which have brought positive effects on reducing air pollutant concentrations [53,55]. A zero-emission zone (ZEZ), only allowing access to zero-emission vehicles also reduce CO_2 emissions dramatically [56]. Enterprises with low energy consumption and high technologies should gain support. Moreover, highway tolls are another effective way to reduce air pollution in Chinese cities [57]. The government should pay great attention to the role of the public in environmental governance [58]. Similar to other studies [46], our study shows that setting travel restrictions also helps improving air quality.

The Random Forest model indicates a strong link between road traffic and NO_2 concentration. This shows that it is feasible to reduce the air pollution by controlling road traffic. Nevertheless, it needs to be carefully evaluated since the effect of reducing the pollutant level by controlling traffic has a certain threshold. Among different road traffic control policy, the thresholds of controlling all kinds of human mobility and the mobility within the city are 70%, higher than the threshold of controlling the human mobility out of and into the city (which is 60%). This means the former two measures can be used for longer term. Moreover, the former two measures have relatively high variation rates before the reduction in human mobility reaches 40%. When the reduction is beyond 20%, the variation rate in the last measure is less than 10. Controlling the human mobility within the city is more effective than controlling the mobility out of and into the city and more efficient than overall control of all kinds of human mobility. Overall, the control of the road traffic in the city has an obvious and efficient effect on the NO_2 concentration.

4.3. Limitations and Future Directiosn

It should be noted that in the past few years, China has implemented new environmental regulations and actively promoted end-of-pipe treatment and industrial structure optimization [33,59]. Therefore, the actual value of the NO_2 concentration in the case of no COVID-19 lockdown may be slightly different from the predicted value the NO_2 concentration calculated using the 2019 model.

The impact of this trend can be optimized by using the relevant data in 2018 or even earlier in future research. In addition, the relationship between anthropogenic activities with different travel purposes and air pollutants could be further analyzed with Google mobility data [60]. Although there is difficulty in finding the same contribution rate of pollution sources in different cities [27], it will be meaningful to make a comparison between many cities in different areas.

5. Conclusions

In this study, we curated datasets on air pollutants, meteorological conditions and human mobility to model the contributions of relevant factors for the changes of air pollution before, during and after the COVID-19 lockdown. Using the Random Forest models, we established sensitivity experiments to estimate quantitatively the relative contributions of the meteorological conditions, human mobility and emissions from industry and households. In addition, we also implemented a predictor to find an effective way to reduce the air pollution by controlling specific kinds of human mobility. The conclusions are as follows:

1. The COVID-19 lockdown led to a significant decrease in the NO_2 concentration. Among the five air pollutants, the change of NO_2 concentration was the most prominent, dropping by 24.9% in the pre-lockdown period, 53.9% in the lockdown period and 15.4% in the post-pandemic period. The average $PM_{2.5}$ concentration and average SO_2 concentration also were the lowest in the 2020 and highest in the 2019. In contrast, the average O_3 concentration increased in 2020 and dropped in 2021.
2. Different air pollutants mechanisms were implied during the four periods. In the pre-pandemic and post-pandemic period, meteorological conditions (wind speed), human mobility (Within-City Migration Index) and emissions from industry and households played a more important role in the simulation of air pollutants. However, road traffic decreased sharply in the pre-lockdown and lockdown period and so they were excluded from the stepwise multiple linear model.

3. Road traffic dominated the reduction in the NO_2 concentration in the lockdown period, with 73.3% reduction caused by human mobility, only 10.0% by meteorological conditions, and 16.7% by emissions from industry and households.
4. When it comes to making policies on road traffic for reducing air pollution, placing an appropriate restriction on human mobility within the city is the most effective way to reduce the air pollution. It functions better when the restriction is below 40% and reaches a cap when the level of human mobility is restricted to 70% or more.

Author Contributions: Conceptualization, Jiansheng Wu, Yun Qian and Yuan Wang; Writing—Review & Editing, Jiansheng Wu, Yuan Wang and Na Wang; Conceptualization, Yun Qian and Yuan Wang; Methodology, Yun Qian; Writing—Original Draft, Yun Qian; Visualization, Yun Qian; Validation, Yuan Wang and Na Wang; Funding acquisition, Jiansheng Wu. All authors have read and agreed to the published version of the manuscript.

Funding: This research was funded by the Shenzhen Fundamental Research Program (No. GXWD20201231165807007-20200816003026001).

Data Availability Statement: The data presented in this study are openly available. The dataset of hourly concentrations of air pollutants can be downloaded from the web-site https://quotsoft.net/air/ (accessed on 5 December 2021). Daily migration data were obtained from Baidu Migration https://qianxi.baidu.com/ (accessed on 5 December 2021). The daily surface climate dataset of Wuhan can be downloaded from the China meteorological science data sharing service network (http://data.cma.cn (accessed on 5 December 2021)).

Conflicts of Interest: The authors declare no conflict of interest.

References

1. Isaifan, R.J. The dramatic impact of Coronavirus outbreak on air quality: Has it saved as much as it has killed so far? *Glob. J. Environ. Sci. Manag.* **2020**, *6*, 275–288. [CrossRef]
2. Shekarrizfard, M.; Faghih-Imani, A.; Tetreault, L.F.; Yasmin, S.; Reynaud, F.; Morency, P.; Plante, C.; Drouin, L.; Smargiassi, A.; Eluru, N.; et al. Regional assessment of exposure to traffic-related air pollution: Impacts of individual mobility and transit investment scenarios. *Sustain. Cities Soc.* **2017**, *29*, 68–76. [CrossRef]
3. Tang, J.Y.; McNabola, A.; Misstear, B. The potential impacts of different traffic management strategies on air pollution and public health for a more sustainable city: A modelling case study from Dublin, Ireland. *Sustain. Cities Soc.* **2020**, *60*, 102229. [CrossRef]
4. Wang, X.X.; Yang, X.M.; Wang, X.F.; Zhao, J.H.; Hu, S.E.; Lu, J.F. Effect of reversible lanes on the concentration field of road-traffic-generated fine particulate matter (PM2.5). *Sustain. Cities Soc.* **2020**, *62*, 102389. [CrossRef]
5. Sohrabi, C.; Alsafi, Z.; O'Neill, N.; Khan, M.; Kerwan, A.; Al-Jabir, A.; Iosifidis, C.; Agha, R. World Health Organization declares global emergency: A review of the 2019 novel coronavirus (COVID-19). *Int. J. Surg.* **2020**, *76*, 71–76. [CrossRef] [PubMed]
6. Wang, C.; Horby, P.W.; Hayden, F.G.; Gao, G.F. A novel coronavirus outbreak of global health concern. *Lancet* **2020**, *395*, 496. [CrossRef]
7. Chen, S.M.; Yang, J.T.; Yang, W.Z.; Wang, C.; Barnighausen, T. COVID-19 control in China during mass population movements at New Year. *Lancet* **2020**, *395*, 764–766. [CrossRef]
8. Fan, Z.Y.; Zhan, Q.M.; Yang, C.; Liu, H.M.; Zhan, M. How Did Distribution Patterns of Particulate Matter Air Pollution (PM(2.5)and PM10) Change in China during the COVID-19 Outbreak: A Spatiotemporal Investigation at Chinese City-Level. *Int. J. Environ. Res. Public Health* **2020**, *17*, 6274. [CrossRef]
9. Tian, H.Y.; Liu, Y.H.; Li, Y.D.; Wu, C.H.; Chen, B.; Kraemer, M.U.G.; Li, B.Y.; Cai, J.; Xu, B.; Yang, Q.Q.; et al. An investigation of transmission control measures during the first 50 days of the COVID-19 epidemic in China. *Science* **2020**, *368*, 638–642. [CrossRef]
10. Huang, G.Y.; Sun, K. Non-negligible impacts of clean air regulations on the reduction of tropospheric NO_2 over East China during the COVID-19 pandemic observed by OMI and TROPOMI. *Sci. Total Environ.* **2020**, *745*, 141023. [CrossRef]
11. Lau, H.; Khosrawipour, V.; Kocbach, P.; Mikolajczyk, A.; Schubert, J.; Bania, J.; Khosrawipour, T. The positive impact of lockdown in Wuhan on containing the COVID-19 outbreak in China. *J. Travel Med.* **2020**, *27*. [CrossRef]
12. He, G.J.; Pan, Y.H.; Tanaka, T. The short-term impacts of COVID-19 lockdown on urban air pollution in China. *Nat. Sustain.* **2020**, *3*, 1005–1011. [CrossRef]
13. Wang, Z.; Uno, I.; Yumimoto, K.; Itahashi, S.; Chen, X.S.; Yang, W.Y.; Wang, Z.F. Impacts of COVID-19 lockdown, Spring Festival and meteorology on the NO_2 variations in early 2020 over China based on in-situ observations, satellite retrievals and model simulations. *Atmos. Environ.* **2021**, *244*, 117972. [CrossRef] [PubMed]
14. Bauwens, M.; Compernolle, S.; Stavrakou, T.; Muller, J.F.; Van Gent, J.; Eskes, H.; Levelt, P.F.; Van der A, R.; Veefkind, J.P.; Vlietinck, J.; et al. Impact of Coronavirus Outbreak on NO(2)Pollution Assessed Using TROPOMI and OMI Observations. *Geophys. Res. Lett.* **2020**, *47*, e2020GL087978. [CrossRef]

15. Gautam, S. COVID-19: Air pollution remains low as people stay at home. *Air Qual Atmos Health* **2020**, *13*, 853–857. [CrossRef] [PubMed]
16. Liu, Q.; Harris, J.T.; Chiu, L.S.; Sun, D.L.; Houser, P.R.; Yu, M.Z.; Duffy, D.Q.; Little, M.M.; Yang, C.W. Spatiotemporal impacts of COVID-19 on air pollution in California, USA. *Sci. Total Environ.* **2021**, *750*, 141592. [CrossRef] [PubMed]
17. Huang, X.; Ding, A.J.; Gao, J.; Zheng, B.; Zhou, D.R.; Qi, X.M.; Tang, R.; Wang, J.P.; Ren, C.H.; Nie, W.; et al. Enhanced secondary pollution offset reduction of primary emissions during COVID-19 lockdown in China. *Natl. Sci. Rev.* **2021**, *8*, nwaa137. [CrossRef]
18. Wang, Y.J.; Wen, Y.F.; Wang, Y.; Zhang, S.J.; Zhang, K.M.; Zheng, H.T.; Xing, J.; Wu, Y.; Hao, J.M. Four-Month Changes in Air Quality during and after the COVID-19 Lockdown in Six Megacities in China. *Environ. Sci. Technol. Lett.* **2020**, *7*, 802–808. [CrossRef]
19. Lovric, M.; Pavlovic, K.; Vukovic, M.; Grange, S.K.; Haberl, M.; Kern, R. Understanding the true effects of the COVID-19 lockdown on air pollution by means of machine learning. *Environ. Pollut.* **2021**, *274*, 115900. [CrossRef] [PubMed]
20. Liu, S.S.; Kong, G.W.; Kong, D.M. Effects of the COVID-19 on Air Quality: Human Mobility, Spillover Effects, and City Connections. *Environ. Resour. Econ.* **2020**, *76*, 635–653. [CrossRef]
21. Sarfraz, M.; Shehzad, K.; Farid, A. Gauging the air quality of New York: A non-linear Nexus between COVID-19 and nitrogen dioxide emission. *Air Qual. Atmos. Health* **2020**, *13*, 1135–1145. [CrossRef] [PubMed]
22. Breiman, L. Random forests. *Mach. Learn.* **2001**, *45*, 5–32. [CrossRef]
23. Kaminska, J.A. The use of random forests in modelling short-term air pollution effects based on traffic and meteorological conditions: A case study in Wroclaw. *J. Environ. Manag.* **2018**, *217*, 164–174. [CrossRef]
24. Grange, S.K.; Carslaw, D.C.; Lewis, A.C.; Boleti, E.; Hueglin, C. Random forest meteorological normalisation models for Swiss PM10 trend analysis. *Atmos. Chem. Phys.* **2018**, *18*, 6223–6239. [CrossRef]
25. Yazdi, M.D.; Kuang, Z.; Dimakopoulou, K.; Barratt, B.; Suel, E.; Amini, H.; Lyapustin, A.; Katsouyanni, K.; Schwartz, J. Predicting Fine Particulate Matter (PM2.5) in the Greater London Area: An Ensemble Approach using Machine Learning Methods. *Remote. Sens.* **2020**, *12*, 914. [CrossRef]
26. Ghude, S.D.; Kulkarni, S.H.; Jena, C.; Pfister, G.G.; Beig, G.; Fadnavis, S.; Van der A, R.J. Application of satellite observations for identifying regions of dominant sources of nitrogen oxides over the Indian Subcontinent. *J. Geophys. Res. Atmos.* **2013**, *118*, 1075–1089. [CrossRef]
27. Xin, Y.; Shao, S.; Wang, Z.; Xu, Z.; Li, H. COVID-2019 Lockdown in Beijing: A Rare Opportunity to Analyze the Contribution Rate of Road Traffic to Air Pollutants. *Sustain. Cities Soc.* **2021**, *75*, 102989. [CrossRef]
28. Yang, J.N.; Wen, Y.F.; Wang, Y.; Zhang, S.J.; Pinto, J.P.; Pennington, E.A.; Wang, Z.; Wu, Y.; Sander, S.P.; Jiang, J.H.; et al. From COVID-19 to future electrification: Assessing traffic impacts on air quality by a machine-learning model. *Proc. Natl. Acad. Sci. USA* **2021**, *118*, e2102705118. [CrossRef]
29. Liu, B.M.; Ma, Y.Y.; Gong, W.; Zhang, M. Observations of aerosol color ratio and depolarization ratio over Wuhan. *Atmos Pollut. Res.* **2017**, *8*, 1113–1122. [CrossRef]
30. Ma, Y.L.; Zhao, Y.D.; Liu, J.T.; He, X.T.; Wang, B.; Fu, S.H.; Yan, J.; Niu, J.P.; Zhou, J.; Luo, B. Effects of temperature variation and humidity on the death of COVID-19 in Wuhan, China. *Sci. Total Environ.* **2020**, *724*, 138226. [CrossRef]
31. Sulaymon, I.D.; Zhang, Y.X.; Hopke, P.K.; Zhang, Y.; Hua, J.X.; Mei, X.D. COVID-19 pandemic in Wuhan: Ambient air quality and the relationships between criteria air pollutants and meteorological variables before, during, and after lockdown. *Atmos. Res.* **2021**, *250*, 105362. [CrossRef] [PubMed]
32. Copat, C.; Cristaldi, A.; Fiore, M.; Grasso, A.; Zuccarello, P.; Santo Signorelli, S.; Conti, G.O.; Ferrante, M. The role of air pollution (PM and NO_2) in COVID-19 spread and lethality: A systematic review. *Environ. Res.* **2020**, *191*, 110129. [CrossRef] [PubMed]
33. Zheng, J.L.; Mi, Z.F.; Coffman, D.; Milcheva, S.; Shan, Y.L.; Guan, D.B.; Wang, S.Y. Regional development and carbon emissions in China. *Energy Econ.* **2019**, *81*, 25–36. [CrossRef]
34. Kraemer, M.U.G.; Yang, C.H.; Gutierrez, B.; Wu, C.H.; Klein, B.; Pigott, D.M.; du Plessis, L.; Faria, N.R.; Li, R.R.; Hanage, W.P.; et al. The effect of human mobility and control measures on the COVID-19 epidemic in China. *Science* **2020**, *368*, 493–497. [CrossRef] [PubMed]
35. Nirel, R.; Dayan, U. On the ratio of sulfur dioxide to nitrogen oxides as an indicator of air pollution sources. *J. Appl. Meteorol.* **2001**, *40*, 1209–1222. [CrossRef]
36. Zhao, P.G.; Tuygun, G.T.; Li, B.L.; Liu, J.; Yuan, L.; Luo, Y.; Xiao, H.; Zhou, Y.J. The effect of environmental regulations on air quality: A long-term trend analysis of SO_2 and NO_2 in the largest urban agglomeration in southwest China. *Atmos. Pollut. Res.* **2019**, *10*, 2030–2039. [CrossRef]
37. Grange, S.K.; Farren, N.J.; Vaughan, A.R.; Rose, R.A.; Carslaw, D.C. Strong Temperature Dependence for Light-Duty Diesel Vehicle NOx Emissions. *Environ. Sci. Technol.* **2019**, *53*, 6587–6596. [CrossRef] [PubMed]
38. Gatti, R.C.; Velichevskaya, A.; Tateo, A.; Amoroso, N.; Monaco, A. Machine learning reveals that prolonged exposure to air pollution is associated with SARS-CoV-2 mortality and infectivity in Italy. *Environ. Pollut.* **2020**, *267*, 115471. [CrossRef]
39. Grange, S.K.; Carslaw, D.C. Using meteorological normalisation to detect interventions in air quality time series. *Sci. Total Environ.* **2019**, *653*, 578–588. [CrossRef] [PubMed]
40. Zhang, W.J.; Wang, H.; Zhang, X.Y.; Peng, Y.; Zhong, J.T.; Zhao, Y.F. Evaluating the contributions of changed meteorological conditions and emission to substantial reductions of PM2.5 concentration from winter 2016 to 2017 in Central and Eastern China. *Sci. Total Environ.* **2020**, *716*, 136892. [CrossRef] [PubMed]

41. Chen, J.X.; Hu, H.; Wang, F.F.; Zhang, M.; Zhou, T.; Yuan, S.C.; Bai, R.Q.; Chen, N.; Xu, K.; Huang, H. Air quality characteristics in Wuhan (China) during the 2020 COVID-19 pandemic. *Environ. Res.* **2021**, *195*, 110879. [CrossRef]
42. Niu, Z.; Hu, T.T.; Kong, L.; Zhang, W.Q.; Rao, P.H.; Ge, D.F.; Zhou, M.G.; Duan, Y.S. Air-pollutant mass concentration changes during COVID-19 pandemic in Shanghai, China. *Air Qual. Atmos. Health* **2021**, *14*, 523–532. [CrossRef]
43. Li, J.W.; Ye, Q.Q.; Deng, X.K.; Liu, Y.L.; Liu, Y.F. Spatial-Temporal Analysis on Spring Festival Travel Rush in China Based on Multisource Big Data. *Sustainability* **2016**, *8*, 1184. [CrossRef]
44. Zhang, J.Y.; Wu, L.Y.; Yuan, F.; Dou, J.J.; Miao, S.G. Mass human migration and Beijing's urban heat island during the Chinese New Year holiday. *Sci. Bull.* **2015**, *60*, 1038–1041. [CrossRef]
45. Hua, J.X.; Zhang, Y.X.; de Foy, B.; Mei, X.D.; Shang, J.; Feng, C. Competing PM2.5 and NO_2 holiday effects in the Beijing area vary locally due to differences in residential coal burning and traffic patterns. *Sci. Total Environ.* **2021**, *750*, 141575. [CrossRef]
46. Biswal, A.; Singh, V.; Singh, S.; Kesarkar, A.P.; Ravindra, K.; Sokhi, R.S.; Chipperfield, M.P.; Dhomse, S.S.; Pope, R.J.; Singh, T.; et al. COVID-19 lockdown-induced changes in NO_2 levels across India observed by multi-satellite and surface observations. *Atmos. Chem. Phys.* **2021**, *21*, 5235–5251. [CrossRef]
47. Xu, W.Y.; Zhao, C.S.; Ran, L.; Deng, Z.Z.; Liu, P.F.; Ma, N.; Lin, W.L.; Xu, X.B.; Yan, P.; He, X.; et al. Characteristics of pollutants and their correlation to meteorological conditions at a suburban site in the North China Plain. *Atmos. Chem. Phys.* **2011**, *11*, 4353–4369. [CrossRef]
48. Liu, B.M.; Ma, Y.Y.; Gong, W.; Zhang, M.; Yang, J. Study of continuous air pollution in winter over Wuhan based on ground-based and satellite observations. *Atmos. Pollut. Res.* **2018**, *9*, 156–165. [CrossRef]
49. Jayamurugan, R.; Kumaravel, B.; Palanivelraja, S.; Chockalingam, M.P. Influence of Temperature, Relative Humidity and Seasonal Variability on Ambient Air Quality in a Coastal Urban Area. *Int. J. Atmos. Sci.* **2013**, *2013*, 264046. [CrossRef]
50. Qiu, H.; Yu, I.T.S.; Wang, X.R.; Tian, L.W.; Tse, L.A.; Wong, T.W. Season and humidity dependence of the effects of air pollution on COPD hospitalizations in Hong Kong. *Atmos. Environ.* **2013**, *76*, 74–80. [CrossRef]
51. Panteliadis, P.; Strak, M.; Hoek, G.; Weijers, E.; van der Zee, S.; Dijkema, M. Implementation of a low emission zone and evaluation of effects on air quality by long-term monitoring. *Atmos. Environ.* **2014**, *86*, 113–119. [CrossRef]
52. Jiang, W.; Boltze, M.; Groer, S.; Scheuvens, D. Impacts of low emission zones in Germany on air pollution levels. *Transp. Res. Procedia* **2017**, *25*, 3374–3386. [CrossRef]
53. Salas, R.; Perez-Villadoniga, M.J.; Prieto-Rodriguez, J.; Russo, A. Were traffic restrictions in Madrid effective at reducing NO_2 levels? *Transport Res. D-Transp. Environ.* **2021**, *91*, 102689. [CrossRef]
54. Ye, J.J.; Qin, Z.L.; Chen, X.G. Adapt by adopting cleaner vehicles?—Evidence from a low-emission zone policy in Nanchang, China. *China Econ. Rev.* **2021**, *66*, 101598. [CrossRef]
55. Bernardo, V.; Fageda, X.; Flores-Fillol, R. Pollution and congestion in urban areas: The effects of low emission zones. *Econ. Transp.* **2021**, *26–27*, 100221. [CrossRef]
56. de Bok, M.; Tavasszy, L.; Kourounioti, I.; Thoen, S.; Eggers, L.; Nielsen, V.M.; Streng, J. Simulation of the Impacts of a Zero-Emission Zone on Freight Delivery Patterns in Rotterdam. *Transp. Res. Rec.* **2021**, *2675*, 776–785. [CrossRef]
57. Fu, S.H.; Gu, Y.Z. Highway toll and air pollution: Evidence from Chinese cities. *J. Environ. Econ. Manag.* **2017**, *83*, 32–49. [CrossRef]
58. Song, Y.; Li, Z.R.; Liu, J.; Yang, T.T.; Zhang, M.; Pang, J.R. The effect of environmental regulation on air quality in China: A natural experiment during the COVID-19 pandemic. *Atmos. Pollut. Res.* **2021**, *12*, 21–30. [CrossRef]
59. Wang, Y.Z.; Hang, Y.; Wang, Q.W.; Zhou, D.Q.; Su, B. Cleaner production vs end-of-pipe treatment: Evidence from industrial SO_2 emissions abatement in China. *J. Environ. Manag.* **2021**, *277*, 111429. [CrossRef]
60. Archer, C.L.; Cervone, G.; Golbazi, M.; Al Fahel, N.; Hultquist, C. Changes in air quality and human mobility in the USA during the COVID-19 pandemic. *Bull. Atmos. Sci. Technol.* **2020**, *1*, 491–514. [CrossRef]